Article

Statistical Analysis and Thermodynamic Equilibrium Modelling for Chemical Composition of Groundwater and Spring Water at Jeju Island, South Korea

Byeong Dae Lee [1], Chan Ho Jeong [2,*], Yong Cheon Lee [2,*] [iD], Yu Jin Lee [2], Jae Ha Yang [3], Chang Oh Choo [4], Hyeon Woo Jang [2], Yong Hwa Oh [1] and Jin Woo Hong [2]

[1]   Groundwater Research Center, Korea Institute of Geoscience and Mineral Resources, Daejeon 34132, Korea; blee@kigam.re.kr (B.D.L.); yonghwa.oh@gmail.com (Y.H.O.)
[2]   Department of Construction and Disaster Prevention Engineering, Daejeon University, Daejeon 34520, Korea; geoabby20@naver.com (Y.J.L.); jhwtime@gmail.com (H.W.J.); jinwoo_hong@naver.com (J.W.H.)
[3]   EGI Consulting Co., Incheon 22698, Korea; egiconsl@gmail.com
[4]   Department of Earth and Environmental Sciences, Andong National University, Andong 36729, Korea; mineralogy@hanmail.net
[*]   Correspondence: chjeong@dju.kr (C.H.J.); dydcjs159@naver.com (Y.C.L.); Tel.: +82-42-280-2573 (C.H.J.); +82-10-2908-0057 (Y.C.L.)

Abstract: The purpose of this study is to delineate the main contributions controlling the chemical composition of groundwater and spring water samples at Jeju Island, South Korea. Groundwater and spring water can be grouped as three chemical types: Fresh water (Ca, Na-HCO_3), sea water mixing (Na-Cl, SO_4) and contamination (Ca-NO_3, Cl). By factor analysis, three factors can explain about 87% of chemical variances: Factor 1 (Na^+ and Cl^-), factor 2 (NO_3^-), and factors 3 (HCO_3^-), which are regarded as indicative ions of sea water mixing, contamination and mineral-water interaction, respectively. Sea water intrusion in the southeastern area of Jeju Island is due to downward distribution of Seogwipo Formation, which plays a role as an aquiclude preventing sea water intrusion in other areas, under sea level at the southeastern coastal area. Nitrate contamination is likely to be affected by pollution sources, i.e., agricultural activities, horse farms and municipal sewage. Thermodynamic saturation index indicates that most of waters are undersaturated with respect to major minerals, which may result from insufficient reaction time within a permeable aquifer. The unsaturation state corresponds to low load scores of Ca, Mg, Na, K, and SiO_2 in factor 3, which means a low contribution of mineral-water interaction.

Keywords: chemical composition; contamination; factor analysis; groundwater; kriging; sea water intrusion; spring water; saturation indices

1. Introduction

Jeju volcanic island is located at the margin of the southwestern part in Korean Peninsula (Figure 1a). Jeju Island, which has been known as an attractive natural reserve area and beautiful scene, was designated as world natural heritage at 2007 by United National Educational, Scientific and Cultural Organization (UNESCO). Tourists greatly increased from 5.8 million in 2008 to 15 million in 2019. For last 50 years, the population of Jeju Island has steadily increased from 358,085 in 1970 to 692,032 in 2018. Water demand has been persistently increased from 146 thousand ton in 2008 to 212.5 thousand ton in 2017 along with the increase of population and tourists [1,2].

Although the island has been known as having the heaviest amount of rainfall (av. 1700 mm/year) in Korean Peninsula during last several ten years, surface water resources are always insufficient

due to the hydrogeological characteristic of highly porous volcanic rocks, where a large amount of rainfall rapidly infiltrates into a permeable underground layer. In the mountainous area of Jeju Island, available water resources are always lacked, while many spring waters yield along the coastal area. Hence, the spring water has been used as a drinking water for a long time before a deep groundwater development until the 1970s. However, spring water along coastal area had also a problem such as sea water mixing, which can cause inappropriate quality as a drinking water. After 1970s, although a lot of groundwaters have been developed as a main water resource including a drinking water, a rapid enlargement of potential contamination sources such as many leisure facilities including hotels and golf resorts, agricultural activities and horse farms that are mainly developed along a coastal line and in mid-mountain areas is threatening the quality of groundwater as a drinking water [3].

Previous geochemical and hydrogeological studies related with groundwater and spring water in Jeju Island have been carried out by several researchers. Koh et al. (2017) estimated the temporal trends from 1993 to 2012 about the concentrations of NO_3-N and Cl from previous data of more than 3900 groundwater samples in Jeju Island by using the Mann-Kendall trend test and Sen's slope analysis, and also analyzed the groundwater contamination according to the change of land use for the period 1995−2009 [4]. All previous data of nitrate and chloride in groundwater of Jeju Island were collected from rectangle grids of 500 m by 500 m, and these data were arranged in time series order and analyzed using Sen's method [5]. The results showed the upward trend of their concentrations from the early 1990s to the early 2000s. In particular, nitrate content has been increased in the low and mid-mountain areas in western and southern watersheds of the island.

The purpose of this study is to investigate the geological and other contributions controlling chemical composition of groundwater and spring water in Jeju Island by using statistical methods such as box-whisker diagram, correlation and factor analyses and thermodynamic equilibrium calculation. Correlation and factor analyses were applied to better explain the possible processes such as water-mineral interaction, anthropogenic inputs and sea water mixing as the origin of the chemical ions of groundwater and spring water. In particular, thermodynamic equilibrium modelling makes an attempt firstly to assess the saturation state of groundwater and spring water with respect to major minerals of Jeju volcanic rocks. Additionally, we applied firstly the kriging method to represent the degree of mineral-water interaction and hydrochemical evolution of groundwater and spring water based on the result of saturation index.
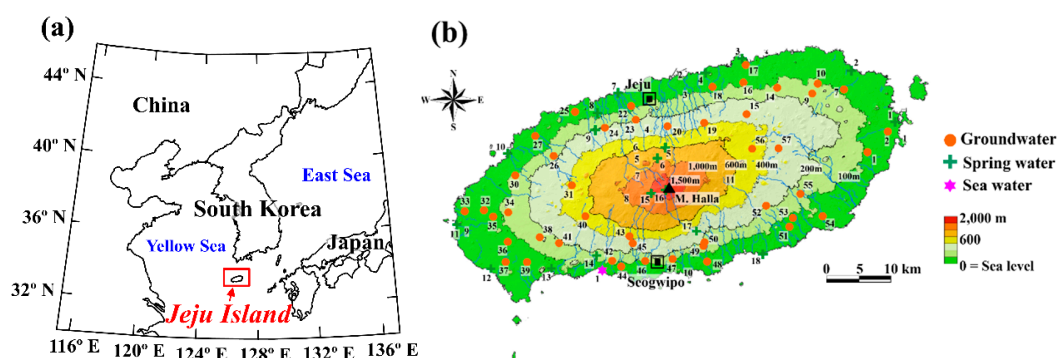

Figure 1. Location map of the study area (Jeju Island) in South Korea (**a**) and location map of groundwater, spring water and sea water samples collected in Jeju Island (**b**).

2. Methods

2.1. Samples and In-Situ Measurement

For this study, groundwater samples in Jeju Island were collected at 38 locations in July and at 47 locations in October, 2016, respectively. 18 spring water samples were also collected in July and October, 2016, respectively. 1 sea water was sampled at southern coastal line in July, 2016. The depth of groundwater wells ranges from −41 to −450 m. The wells are classified into 4 types in view point

of purpose of use; 2 drinking water wells, 12 living water wells, 24 agricultural water wells and 9 observation wells. The location map of water samples is shown in Figure 1b. Measurements of pH, oxidation–reduction potential (Eh), dissolved-oxygen content (DO), electrical conductivity (EC) of all water samples were made in situ while using portable instruments (HM-12P and CM-14P and RM-12P, DKK-TOA Co., Tokyo, Japan) 10–20 min after purging to achieve stable values in case of groundwater. Alkalinity, being expressed as HCO_3^- concentration, was quantified on-site by titration with 0.05 M HCl. All of the water samples were filtered through a 0.45 μm membrane filter and then stored in 60 mL polythene bottles before chemical analyses. Samples for cation analysis were acidified to pH < 2 with ultrapure HNO_3.

2.2. Chemical Analysis

The concentration of the major cations was determined by graphite furnace atomic absorption spectrometry (AAS; PE3100, Perkin-Elmer, Waltham, MA, USA) and inductively coupled plasma–atomic emission spectrometry (ICP–AES; JY-38plus, Jobin Yvon, Longjumeau, France). The contents of major anions were analyzed by ion chromatography (IC; Dx 300, Dionex Co., Sunnyvale, CA, USA). All chemical analyses were conducted at Korea Institute of Geoscience and Mineral Resources (KIGAM). The reliability of the chemical analyses was estimated by calculating the charge imbalances between the cation and anions; the percentage of charge balance was within ±6%.

2.3. Statistical Analysis

The correlation and factor analyses for major ions of groundwater and spring water were applied to understand their relationship among chemical variances. In particular, factor analysis was performed to extract major factors having highly loaded eigenvalues of chemical variances. IBM Statistical Package for Social Sciences (Armonk, NY, USA), version 25 analysis software was used for this statistical analysis [6]. R-mode factor analyses were performed as principal components after Varimax rotation, which allowed verification of factor loadings related to percentages of the total variance within the data.

2.4. Thermodynamic Modeling

The saturation index (SI) was calculated to define the state of thermodynamic equilibrium between potential reactive minerals and secondary minerals and groundwater and spring water by using a software program PHREEQC (Denver, CO, USA) [7,8]. The equilibrium calculation was supported by thermodynamic equilibrium constant installed at WATEQ4F data base. The calculation procedure can be converged using Newton-Raphson iteration method.

3. Study Area

Jeju Island is a Tertiary volcanic island of 1847 km^2 area with an elliptical shape of 74 km in a long diameter and a short diameter of 32 km. Mt. Halla, the highest peak located at the central part of the island, rises 1950 m above sea level. Jeju Island has a mild oceanic climate throughout the year with a narrow annual temperature variation. Annual mean temperature and precipitation of Jeju Island from 2009 to 2018 are 17.1 °C and 1704 mm/year, respectively. Precipitation in the Mt. Halla in the central area of the island is over two times as large as the coastal area. Over about 60 percent of annual precipitation occurs during the monsoon season from June to September, which is a common weather characteristic for eastern Asia [9].

The geologic map of Jeju Island is shown in Figure 2a [10]. The island is mainly composed of porous volcanic lava flows formed from multiple eruptions that occurred from the late Pliocene to the Quaternary period, with less sedimentary rocks imbedded between volcanic rocks. The volcanic rocks of the island are known as basalt, trachybasalt, basaltic trachyandesite, trachyandesite and trachyte. The geochemical studies supported that the volcanic rocks have characteristics of oceanic island basalt and the eruption which is the hot-spot related to the mantle-plumes [11]. Seogwipo Formation which is distributed under volcanic rock consists of gravelly sandstone, sandstone, sandy mudstone and

mudstone, characterized by abundant bioclastic shells [12–14]. Figure 2b shows the simplified geologic cross section (A–A') of Figure 2a. Underneath the Seogwipo Formation, the Unconsolidated Formation (U Formation), which is composed of unconsolidated sediments such as gray to light gray fine sand and silt, and the basement of granite are located sequentially [15]. As shown in Figure 1b, three types of groundwater exist on Jeju Island; high level, parabasal, and basal groundwater according to their depth and seawater mixing [16,17]. High-level groundwater occurs only at high-altitude areas and has no contact with seawater. Basal groundwater mixed with sea water exist in the eastern part of cross section. The elevation of the Seogwipo Formation plays a role to determine the location and shape of the freshwater and seawater interface, which differs from the east coast to the west coast (Figure 1b). The Seogwipo Formation with a low permeability acts as an aquiclude in other areas without southeastern coastal area [16,18].
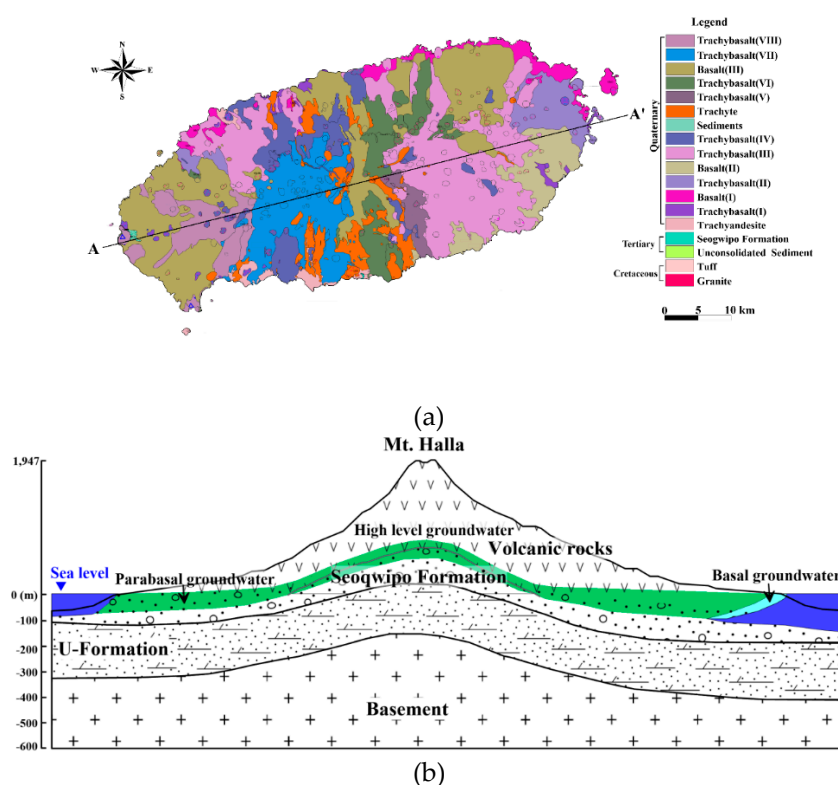

(a)

(b)

Figure 2. Geologic map (**a**) and simplified geologic cross section (A–A') including three aquifer types of groundwater (**b**) of Jeju Island [4,10].

Based on the drilled core data and water level data from total 203 wells, Kim et al. (2011) suggested that main aquifers are the clinkers and fracture zones developed in feldspar olivine basalt, acicular feldspar olivine basalt, feldspar augite olivine basalt, augite olivine basalt, aphanitic basalt, trachyandesite, trachybasalt, feldspar augite basalt, feldspar basalt and hyaloclastite within Seogwipo Formation [19]. Basaltic rocks are known to be highly permeable with hydraulic conductivity in the range 84.6 to 552.2 m/d [15,16,20]. In consequence of the highly permeable layer, groundwater recharge rate in the island was estimated to be 38.7–45.8 % of the average precipitation [10,20,21]. However, the Seogwipo Formation with a low permeability acts as an aquiclude [16,18]. The data of chlorofluorocarbons (CFCs) as an environmental tracer of groundwater in Jeju Island suggested that the groundwater has a relative young age (15 to 25 year) which indicates a rapid flow in a porous aquifer after the recharge [22]. Tritium age of groundwater was estimated as a residence time from 9.57 to above 40 year with an average age of 17.8 year [23].

The change of land use can be an important factor threatening groundwater quality in Jeju Island. The urban area has been continuously enlarged along the coastal areas below 100 m altitude. The 31

golf resorts of 3361 ha, horse farms of 15,375 ha and tangerine orchards of 20,021 ha, which can be potential pollution sources have been also developed in the areas below 400 m in elevation. However, the mountain areas above 400 m altitude are well conserved as a natural environment.

4. Results and Discussion

4.1. Geochemical Composition and Water Type

The statistical values of in situ measurement data and chemical compositions of groundwater and spring water in Jeju Island are given in Tables 1 and 2, respectively, according to three zones of their occurrence altitude (below 100 m, 100 to 400 m and above 400 m) and sampling months (July and October). The chemical composition of groundwater and spring water can be influenced by the occurrence altitude because groundwater and spring water regionally flow from a higher recharge area including Mt. Halla to a lower discharge area (a coastal area). The potential factors controlling the chemical composition of groundwater and spring water would be mineral compositions of rock contacting along their flow paths, anthropogenic inputs according to land use, and sea water intrusion along a coastal line. The pH, electrical conductivity and major-ion contents of groundwater and spring water are statistically presented in a box-whisker diagram according to two seasons (July and October) and their altitude (<100 m, 100–400 m and 400< m) (Figure 3). The diagram shows a graphical representation of key values (i.e., minimum, 25th percentile, median, 75th percentile and maximum; endpoint is 2.5% and 97.5% of the range). The pH value of groundwater shows a weak alkaline range of median 7.22–7.77, which is a slightly higher range than that of spring water (6.74–6.89). Electrical conductivity of spring water has a higher value than that of groundwater, and an electrical conductivity of groundwater and spring water shows an increasing trend from a high altitude to a low altitude.

The content of Na^+, Cl^- and SO_4^{2-} between spring water and groundwater shows a great difference in low land areas below 100 m elevation, that is, their median concentrations in spring water have much higher values than those of groundwater, whereas their concentrations in a high land area (above 100 m elevation) show the similar range. Na^+, Cl^- and SO_4^{2-} contents of spring water and groundwater in coastal areas amount to maximum 696 mg/L, 1380 mg/L, 185 mg/L, respectively, whereas their maximum concentrations in high land areas decrease greatly below 20 mg/L. This implies the effect of seawater mixing into spring water along the coastal area in addition to the origin from mineral-water interaction. We will discuss further sea water mixing through the correlation and factor analyses in the next section.

HCO_3^- concentration of groundwater and spring water ranges from 3.1 to 240 mg/L, showing an increasing trend from a high land area to a low land area. The natural process such as the dissolution of carbonate minerals, atmospheric and soil CO_2 gas would be major mechanisms to supply HCO_3^- into the groundwater as follows:

$$CaCO_3 + CO_2 + H_2O \leftrightarrow Ca^{2+} + 2HCO_3^-, CO_2 + H_2O \leftrightarrow H^+ + HCO_3^- \tag{1}$$
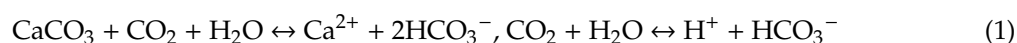
The anthropogenic CO_2 gas as well as a natural origin CO_2 can be supplied from municipal waste site, oxidation of organic materials leaked from old latrines, and sewage system in urban area. In this study, excess carbon dioxide partial pressure ($EpCO_2$), that is the CO_2 content of water samples relative to pure water was introduced to estimate HCO_3^- content originated from anthropogenic CO_2 gas [24,25]:

$$EpCO_2 = \frac{\left(Alk_{Gran\ in\ \frac{\mu Eq}{1unit}} + 10^{6-pH}\right) \times 10^{6-pH} \times \gamma}{(6.46 - 0.0636 \times t°C)} \tag{2}$$

where, γ and t are correction terms for ion activity and temperature (t °C), respectively. For the calculations, γ has been used the values calculated from the PHREEQC program. In situ measured temperature value was used as water temperature in Equation (2).

Table 1. Statistical data of chemical compositions of groundwater samples according to the altitude in Jeju Island (Unit: mg/L).

Altitude (el. m)		Month	Temp (°C)	pH	Eh (mV)	EC (μScm⁻¹)	Na⁺	Ca²⁺	Mg²⁺	K⁺	Sr²⁺	F⁻	Cl⁻	NO₃⁻	SO₄²⁻	HCO₃⁻	SiO₂
<100	Max.	July	20.3	8.44	200	530	70.3	26.2	30.6	8.08	0.08	0.45	114	96.1	27.1	234	40.8
		October	18.7	8.98	241	1136	197	35.1	33.3	16.3	0.15	0.39	397	61.6	57.0	240	40.2
	Min.	July	14.8	6.60	126	97.3	7.74	5.90	2.66	2.49	0.00	0.02	8.63	0.00	1.39	18.3	21.6
		October	14.6	6.70	57.0	109	7.07	4.79	2.61	2.37	0.01	0.02	7.75	0.40	1.59	19.8	22.0
	Ave.	July	17.1	7.34	176	200	17.9	10.9	8.85	4.05	0.02	0.07	24.4	33.7	5.51	46.7	29.3
		October	16.3	7.47	188	227	21.3	11.2	8.09	4.94	0.04	0.06	33.1	24.0	6.63	56.7	31.5
100~400	Max.	July	18.4	7.84	171	172	11.7	10.3	9.11	4.95	0.03	0.06	19.1	43.1	6.01	68.7	35.7
		October	16.5	8.29	278	219	30.9	16.3	9.26	3.41	0.03	0.10	49.2	39.8	7.71	97.6	39.1
	Min.	July	14.3	6.47	156	50.9	5.15	2.94	1.45	1.79	0.00	0.03	2.28	0.00	1.31	8.85	9.58
		October	13.8	6.35	−15	62.3	4.58	2.84	1.69	1.74	0.00	0.03	4.93	0.26	1.29	15.4	2.44
	Ave.	July	16.1	7.22	162	90.1	7.60	5.34	3.98	2.61	0.01	0.04	8.91	11.8	2.46	29.1	26.9
		October	15.4	7.37	178	103	7.91	4.79	3.74	2.41	0.01	0.05	9.69	6.77	2.34	32.7	28.5
400<	Max.	July	15.5	8.18	-	79.0	6.47	4.54	4.50	3.26	0.01	0.05	6.29	0.00	1.62	43.0	32.0
		October	15.4	8.33	188	102	6.00	4.78	5.17	2.68	0.00	0.06	6.31	0.63	1.68	51.9	35.1
	Min.	July	15.1	7.32	-	45.3	4.49	2.97	1.65	1.85	0.00	0.04	4.90	0.00	1.41	22.3	24.6
		October	14.9	7.05	176	59.6	4.30	3.03	1.87	1.76	0.00	0.03	4.91	0.42	1.40	24.4	26.7
	Ave.	July	15.3	7.72	-	63.3	5.57	3.59	2.91	2.48	0.00	0.05	5.68	0.00	1.51	29.9	27.3
		October	15.1	7.77	182	80.7	5.23	3.68	3.19	2.16	0.00	0.05	5.59	0.55	1.53	34.1	29.9

Table 2. Statistical data of chemical compositions of spring water samples according to the altitude in Jeju Island (Unit: mg/L).

| Altitude (el. m)		Month	Temp (°C)	pH	Eh (mV)	EC (μS cm^{-1})	Na$^+$	Ca^{2+}	Mg^{2+}	K$^+$	Sr^{2+}	F$^-$	Cl$^-$	NO$_3^-$	SO$_4^{2-}$	HCO$_3^-$	SiO$_2$
<100	Max.	July	19.2	8.12	-	3510	655	50.1	85.3	35.2	0.22	0.19	1280	200	177	113	42.6
		October	18.6	8.05	237	4490	696	63.3	82.5	36.9	0.24	0.35	1380	205	185	162	43.6
	Min.	July	15.1	6.19	-	133	13.6	6.36	6.9	3.21	0.01	0.04	17.4	21.8	4.48	33.6	18.4
		October	14.8	6.19	146	183	10.5	8.71	7.32	3.05	0.01	0.00	16.3	23.6	4.40	32.0	2.50
	Ave.	July	16.9	6.89	-	931	138	27.0	24.3	12.5	0.09	0.08	259	80.9	45.1	52.3	27.6
		October	17.3	6.94	195	1003	128	23.6	22.6	10.1	0.10	0.08	234	66.2	38.3	63.8	29.8
100~400	Max.	July	16.7	7.02	-	290	15.8	29.1	20.5	1.60	0.14	0.04	34.3	160	4.24	25.0	18.6
		October	16.6	7.54	224	284	13.0	20.5	12.6	6.00	0.09	0.04	25.6	85.0	5.60	41.2	32.9
	Min.	July	14.8	6.70	-	44.4	4.17	3.02	1.76	1.46	0.00	0.00	5.04	4.46	1.89	12.2	17.7
		October	15.4	6.48	188	54.3	3.91	2.50	1.47	1.32	0.01	0.00	3.8	0.93	1.42	22.0	22.2
	Ave.	July	15.8	6.86	-	167	9.99	16.1	11.1	1.53	0.07	0.02	19.7	82.2	3.07	18.6	18.2
		October	16.0	6.92	211	190	9.74	12.0	7.58	2.96	0.05	0.02	16.9	41.3	3.39	33.3	26.0
400<	Max.	July	13.4	7.02	-	39.9	4.36	2.23	1.52	1.02	0.00	0.08	7.39	2.69	2.03	12.2	17.3
		October	13.0	7.55	239	48.8	4.41	2.61	1.73	0.97	0.01	0.08	6.60	2.86	2.00	16.8	20.0
	Min.	July	9.40	6.20	-	9.40	1.35	0.67	0.23	0.46	0.00	0.00	1.58	0.00	0.77	4.58	6.03
		October	10.1	6.37	210	14.2	1.16	0.63	0.18	0.39	0.00	0.00	1.50	0.00	0.90	3.10	7.01
	Ave.	July	11.7	6.74	-	25.5	2.87	1.82	0.93	0.72	0.00	0.03	3.75	0.70	1.39	9.31	10.9
		October	11.4	6.79	224	36.0	2.93	1.93	0.98	0.68	0.00	0.02	3.81	0.99	1.45	11.0	13.4
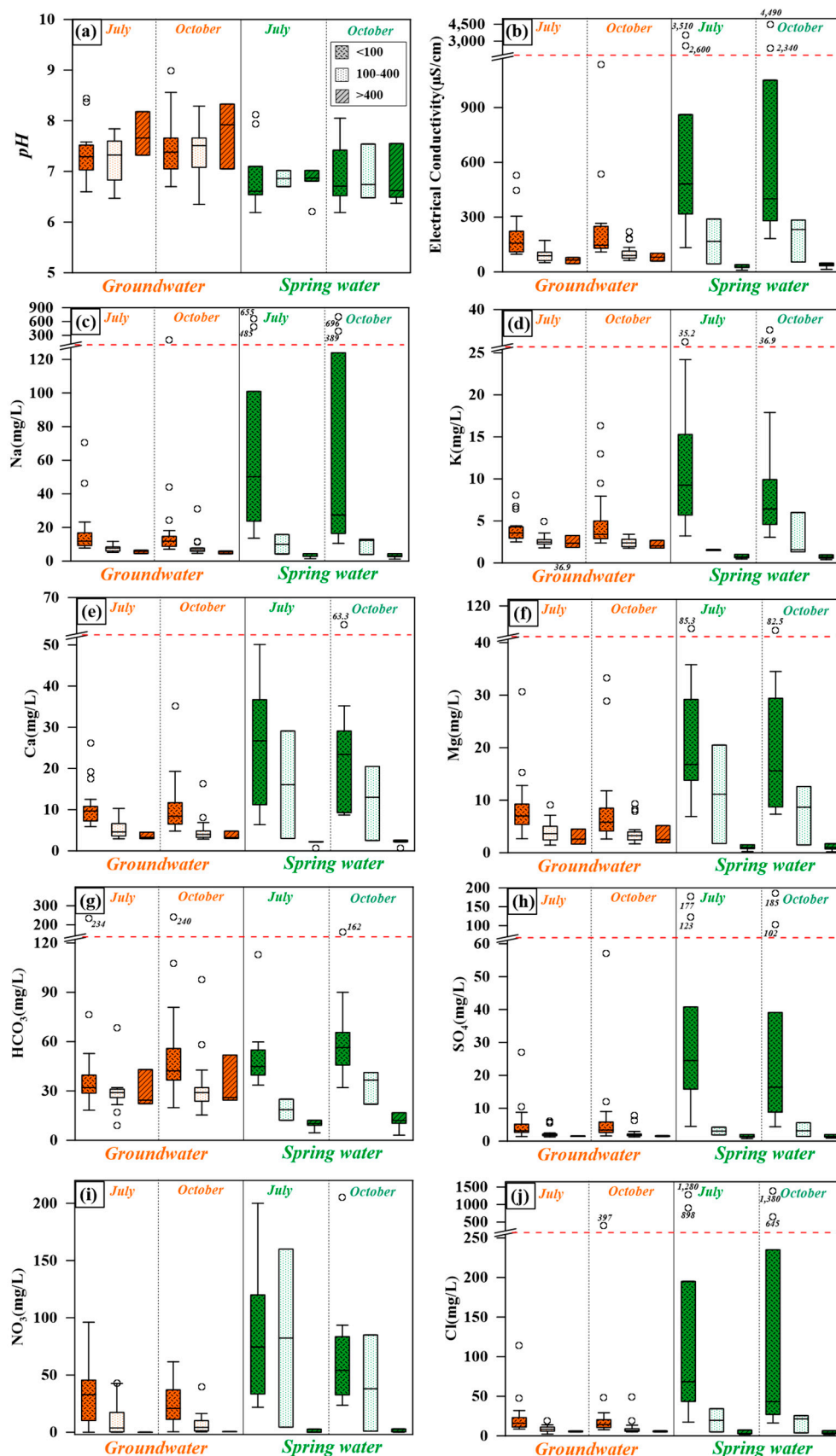
Figure 3. Box-whisker statistical diagrams of pH, electrical conductivity and major ions of groundwater and spring water in Jeju Island. (**a**), (**b**), (**c**), (**d**), (**e**), (**f**), (**g**), (**h**), (**i**) and (**j**) are the variation of pH, EC, Na, K, Ca, Mg, HCO_3, SO_4, NO_3 and Cl as a function of altitude, respectively.

pH endpoint is the pH value from the endpoint of the alkalinity measurement. The endpoint pH is usually 4.3; hence the $10^{(6 - \text{pHendpoint})}$ term is 31.6 μEq/L. In addition, pCO_2, which is closely related with $EpCO_2$ of water sample, was also calculated by the PHREEQC program. The pCO_2 level of soil layer in open system is generally known as the range of $10^{-1.5}$ to $10^{-2.5}$ atm, and atmospheric CO_2 is in the equilibrium state at $10^{-3.5}$ atm [26]. Figure 4a shows the positive relationship between pCO_2 and $EpCO_2$ of groundwater and spring water, and pCO_2 of all water samples except one spring water are below soil pCO_2 range. The very low regression coefficients (R^2, 0.1–0.12) between NO_3 and $EpCO_2$ of groundwater and spring water indicate no distinct relationship (Figure 4b). Thus, this indicates that HCO_3 in water samples was mainly originated from natural reaction or sea water mixing, regardless of the dissolution of CO_2 gas generated from pollution sources.
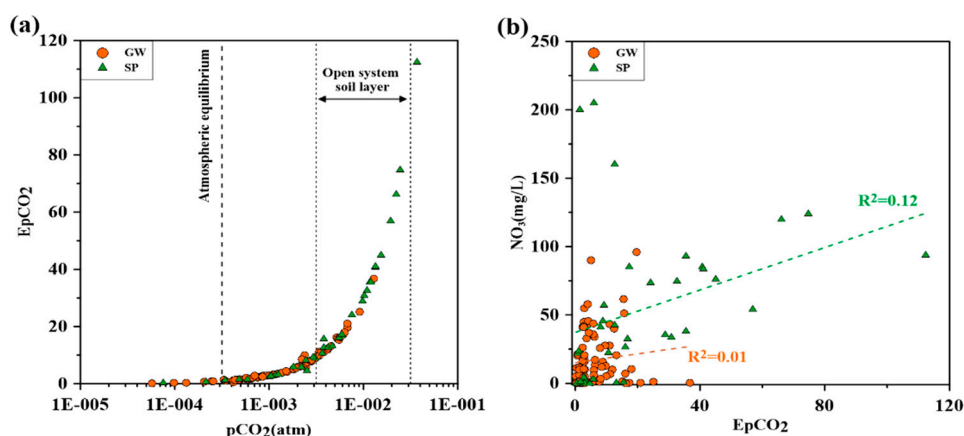

Figure 4. The relationships between pCO_2 and $EpCO_2$ (**a**), and between NO_3 and $EpCO_2$ (**b**).

Nitrate-nitrogen (NO_3-N) contamination of groundwater is major concern for a sustainable use of groundwater resources in many countries [26–32]. Nitrate concentration as a drinking water is regulated to be lower than 45 mg/L as NO_3^- or 10 mg/L as NO_3-N in Korea. The maximum NO_3^- concentrations of groundwater and spring water in Jeju Island amount to 96.1 mg/L and 205 mg/L, respectively. About 50% of spring water exceed the regulation limit (45 mg/L) of NO_3^-. It is assumed that NO_3^- in water samples was mainly derived from pollution sources such as domestic sewage, nitrogen fertilizer of agriculture activity and resort facilities in low and mid-mountain area.

In Figure 3, the statistical range of Ca^{2+}, Mg^{2+} and NO_3^- contents shows a similar trend; (1) their concentrations in spring water below 400 m elevation show higher levels than those in groundwater, (2) their concentration shows an increasing trend from higher areas to lower areas. Such trend implies that Ca and Mg are originated from the common source with nitrate besides the dissolution process of Mg(Ca)-bearing-minerals such as anorthite, augite and olivine of basaltic rocks. We will discuss further their origin through a statistical analysis method in the next section.

To delineate the contamination, sea water mixing and chemical types of groundwater and spring water, major cations and anions (expressed as meq percentiles) are shown in a trilinear plot (Piper diagram; Figure 5). The diagram indicates that the chemical compositions of fresh groundwater and spring water of the Ca (Na)–HCO_3 type have been changed along two different paths: (1) A contamination path (Ca-Cl, NO_3 type), and (2) a sea water mixing path (Na-Cl (SO_4) type). The chemical type coincides with the occurrence altitude of groundwater and spring water, that is, sea water mixing water (Na-Cl (SO_4) type) and contamination water (Ca-Cl, NO_3 type) occur mainly in low land areas (coastal areas), and fresh water of Ca(Na)–HCO_3 type occur mainly in middle and high land (mountain) areas.
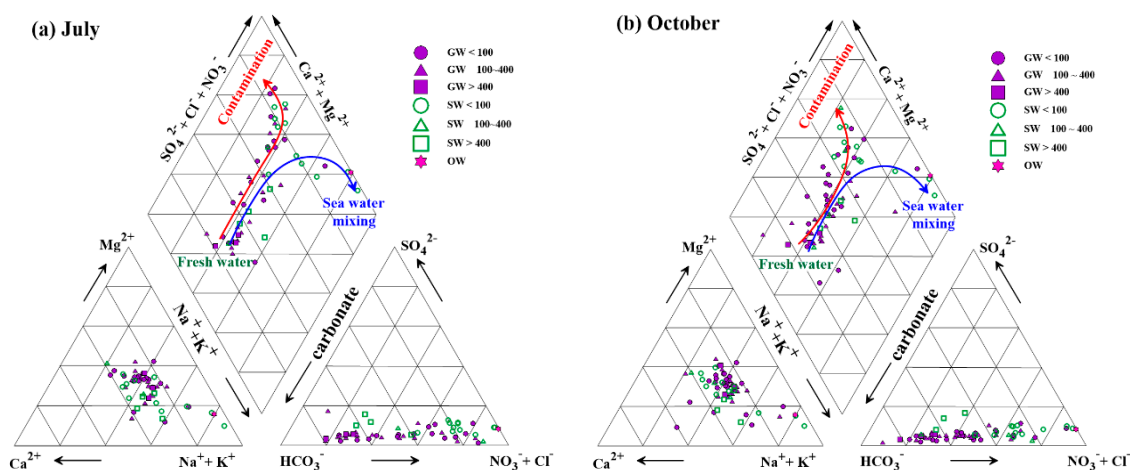
Figure 5. Piper diagram of the major chemical compositions of groundwater (GW, solid symbols), spring water (SW, open symbols) and sea water (OW) expressed in milli-equivalent percentages. (**a**) and (**b**) represent July and October as sampling seasons, respectively.

Figure 6 represents the kriging results of concentrations of NO_3 and Cl, which are the indicators of anthropogenic contamination and sea water mixing of both groundwater and spring water samples, respectively. According to the figure, the concentrations of NO_3 and Cl show a distinct gradation with the occurrence altitude of groundwater and spring water. NO_3 concentration has an increasing trend from high mountain areas toward low coastal areas, with a seasonal variation. The highest content of Cl as an indicator of sea water mixing are restricted at coastal and low areas in the southeastern part of Jeju Island. The restricted sea water intrusion is closely related with the distribution of Seogwipo Formation. The elevation of the Seogwipo Formation plays a role to determine the location and shape of the freshwater and seawater interface, which differs from the east coast to the west coast (Figure 1b). The Seogwipo Formation with a low permeability acts as an aquiclude in other areas except southeastern coastal area [16,18]. The high grade contour of chlorine in the southeastern coastal area of Jeju Island is due to the distribution of Seogwipo Formation under sea water level, which results in sea water intrusion into basal groundwater.
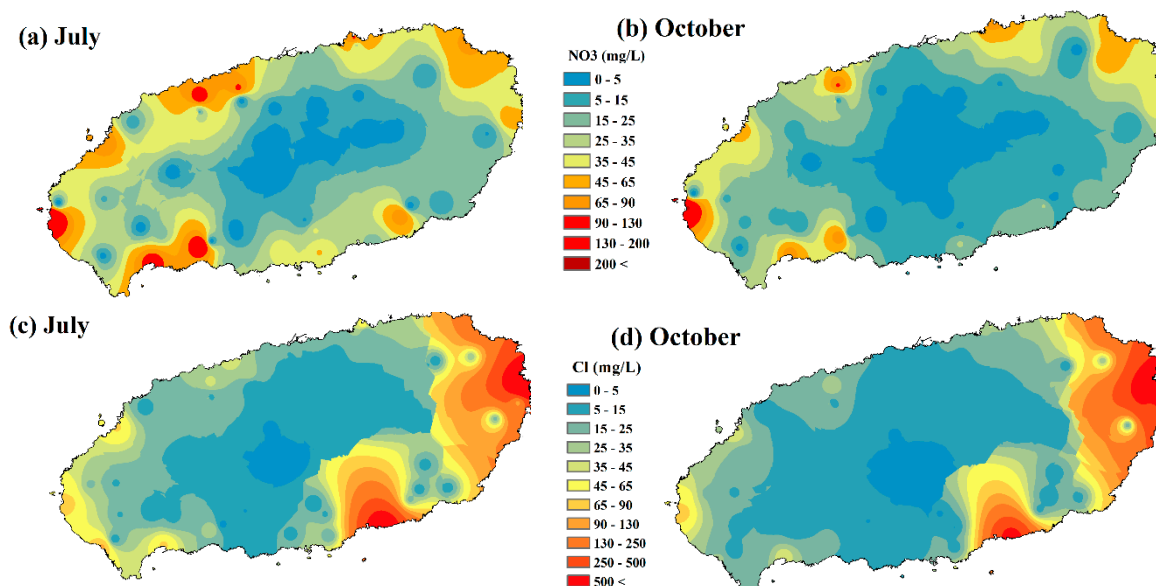

Figure 6. Kriging maps of the NO_3 and Cl contents of groundwater and spring water in Jeju Island. (**a**) and (**b**) represent the kriging maps of NO_3 concentration at July and October, respectively; (**c**) and (**d**) show the kriging maps of Cl concentration at July and October, respectively.

The high NO_3 content is recognized along the northern and the southern coastal areas of the western part of Jeju Island. Nitrate in groundwater and spring water may be primarily derived from pollution sources, i.e., agricultural activities, municipal sewage and horse farms along coastal and low areas. In Figure 6, the difference of NO_3 content contour between July and October is likely to be due to the following dilution effect of heavy rainfall during a monsoon season (June to September). The kriging result of a seasonal variation corresponds to a shorter contamination path line in October than July on the Piper diagram.

4.2. Correlation Analysis and Factor Analysis

The statistical method such as multivariate analysis can be used to characterize its geochemical processes through data reduction and classification with respect to chemical composition of groundwater. When correlation analysis and factor analysis are applied to chemical data of groundwater, dominant processes can be identified as common factors that are sets of variables having strong associations with one another [33–37].

In this study, correlation and factor analyses were used to delineate the possible common sources such as natural chemical weathering, anthropogenic inputs and sea water mixing for the chemical composition of groundwater and spring water. The variables for correlation and factor analyses were Na^+, K^+, Mg^+, Ca^+, HCO_3^-, Cl^-, SO_4^{2-}, NO_3^-, SiO_2, F^-, and Sr^{2+}.

The results of correlation coefficient among major ions of groundwater and spring water are summarized in Table 3. Chlorine as an indicator of sea water mixing has high Pearson's correlation coefficients with Na (0.998), SO_4 (0.989), K (0.901), and Mg (0.882) in order. NO_3 as a representative composition of anthropogenic contamination, shows high correlation coefficients with Ca (0.856) and Sr (0.699). Although the concentration of Ca, Mg and NO_3 shows a similar trend in the box-whisker diagram (Figure 3), however, a correlation coefficient between NO_3 and Mg has a low value of 0.438, which means a low contribution from a common source. HCO_3 originated from natural chemical processes has high to moderate correlation coefficients with F (0.701) and Ca (0.522).

Table 3. The matrix of correlation coefficients among chemical components of groundwater and spring water in Jeju Island.

	Na	Ca	Mg	K	Sr	SiO$_2$	F	Cl	NO$_3$	SO$_4$	HCO$_3$
Na	1	0.324 **	0.879 **	0.904 **	0.478 **	−0.030	0.314 **	0.998 **	0.119	0.990 **	0.095
		0.003	<0.001	<0.001	<0.001	0.747	0.005	<0.001	0.192	<0.001	0.300
Ca	0.324 **	1	0.630 **	0.489 **	0.869 **	0.166	0.191 *	0.322 **	0.856 **	0.393 **	0.522 **
	0.003		<0.001	<0.001	<0.001	0.069	0.036	0.003	<0.001	<0.001	<0.001
Mg	0.879 **	0.630 **	1	0.878 **	0.685 **	0.163	0.363 **	0.882 **	0.438 **	0.891 **	0.359 **
	<0.001	<0.001		<0.001	<0.001	0.075	<0.001	<0.001	<0.001	<0.001	<0.001
K	0.904 **	0.489 **	0.878 **	1	0.575 **	0.093	0.340 **	0.901**	0.265 **	0.924 **	0.269 **
	<0.001	<0.001	<0.001		<0.001	0.311	<0.001	<0.001	0.003	<0.001	0.003
Sr	0.478**	0.869 **	0.685 **	0.575 **	1	0.041	0.141	0.483 **	0.699**	0.529**	0.421**
	<0.001	<0.001	<0.001	<0.001		0.654	0.122	<0.001	<0.001	<0.001	<0.001
SiO$_2$	−0.030	0.166	0.163	0.093	0.041	1	0.183 *	−0.040	0.184 *	−0.040	0.382 **
	0.747	0.069	0.075	0.318	0.654		0.045	0.667	0.043	0.666	<0.001
F	0.314 **	0.191 *	0.363 **	0.340 **	0.141	0.183 *	1	0.269 **	−0.055	0.283**	0.720 **
	0.005	0.036	<0.001	<0.001	0.122	0.045		0.003	0.548	0.002	<0.001
Cl	0.998 **	0.322 **	0.882 **	0.901 **	0.483 **	−0.040	0.269 **	1	0.120	0.989 **	0.069
	<0.001	0.003	<0.001	<0.001	<0.001	0.667	0.003		0.190	<0.001	0.454
NO$_3$	0.119	0.856 **	0.438 **	0.265 **	0.699 **	0.184 *	−0.055	0.120	1	0.192 *	0.203 *
	0.192	<0.001	<0.001	0.003	<0.001	0.043	0.548	0.190		0.035	0.026
SO$_4$	0.990 **	0.393 **	0.891 **	0.924 **	0.529 **	−0.040	0.283 **	0.989 **	0.192 *	1	0.089
	<0.001	<0.001	<0.001	<0.001	<0.001	0.666	0.002	<0.001	0.035		0.334
HCO$_3$	0.095	0.522 **	0.359 **	0.269 **	0.421 **	0.382 **	0.720 **	0.069	0.203*	0.089	1
	0.300	<0.001	<0.001	0.003	<0.001	<0.001	<0.001	0.454	0.026	0.334	

Note: ** ($P < 0.01$), * ($P < 0.05$).

The R-mode factor analysis was applied to obtain correlations among the chemical components of groundwater and spring water samples. Factor analysis was done as follows: The correlation matrix, the array of correlation coefficients for all possible pairs of variables, was calculated. Then, the matrix was diagonalized and its principal components (eigenvectors) were obtained. The so-called factor 1 is related to the largest eigenvalue and is able to explain the greatest amount of variance in the data set. The second factor (orthogonal and uncorrelated with the first one) explains the most of the remaining variance, and so forth [38].

The chemical composition of groundwater and spring water can be determined by potential mechanisms such as natural chemical weathering, anthropogenic inputs and seawater mixing. Hence, the concentration of chemical ions can be loaded by above three partial contributions. Factor analysis was applied to distinguish the main contributions for chemical ions.

Three factors were extracted to statistically represent the contributions influencing chemical composition of groundwater and spring water. The equimax rotation method with Kaise normalization was applied to extract the factors. Three significant factors explain 87% of total sample variance. The variance explanations of the factors are 43.82% for factor 1, 25.11% for factor 2, and 19.17% for factor 3, respectively.

Table 4 shows that variables of Cl, Na, K, SO_4 and Mg have high positive load scores (0.848–0.991) on factor 1, and that the variables of NO_3, Ca and Sr as factor 2 are highly loaded as the value of 0.813–0.946, and HCO_3 and F as factor 3 have positive loadings of 0.833–0.904. Three factors with different factor loads indicate that three contributions are involved in determining the chemical composition of groundwater and spring water with a different ratio. The Cl, NO_3 and HCO_3 have the highest loads on factor 1, 2 and 3, respectively. A high concentration above average Cl content in fresh groundwater and spring water implies strongly sea water intrusion into spring water and groundwater along coastal areas.

Table 4. Equimax factor matrix of geochemical composition and factor scores of groundwater and spring water samples.

Components	Factor1	Factor 2	Factor 3
Na	0.991	0.079	0.025
Cl	0.991	0.089	−0.012
SO_4	0.982	0.158	−0.002
K	0.905	0.244	0.160
Mg	0.848	0.411	0.223
NO_3	0.036	0.946	0.015
Ca	0.253	0.908	0.260
Sr	0.420	0.813	0.134
HCO_3	0.065	0.270	0.904
F	0.315	−0.145	0.833
SiO_2	−0.096	0.144	0.571
Eigenvalue	4.820	2.762	1.998
Cumulative Eigenvalue	4.820	7.582	9.580
% Variance Explained	43.819	25.107	18.167
Cumulative % variance	43.819	68.926	87.093

As described in the previous section, because NO_3 has nothing to do with a lithologic source, it may be primarily introduced by pollution sources, i.e., agricultural activities, municipal sewage and horse farms, etc. From the calculation of pCO_2 and $EpCO_2$ in the previous section, it is evident that HCO_3 is originated by the dissolution of carbonate minerals and atmospheric and soil CO_2. Hence,

factor 1 (Na, Cl and SO$_4$), factor 2 (NO$_3$) and factor 3 (HCO$_3$) are assumed to be indicative ions of sea water mixing, contamination, mineral-water interaction as the main contributions for chemical composition of groundwater and spring water, respectively.

Figure 7 shows the relationship of factor loads among variables of groundwater and spring water. Na, Cl and SO$_4$, NO$_3$ and HCO$_3$ are plotted at each end member of factor 1, 2 and 3, respectively. Although ions such as K, Mg, Ca, SiO$_2$, F and Sr have also high load values within main factor, they have effective load scores in other factors. In Figure 7a, Ca, Sr, Mg and K have effective load values in both sea water mixing (factor 1) and contamination (factor 2), that indicates their origin from two sources with a different ratio. Figure 7b shows that Ca, Mg, K and Sr are plotted in the middle zone between factor 1 and factor 3. K, Mg, Sr, Ca and SiO$_2$ have effective load scores in both factor 2 and factor 3 (Figure 7c).
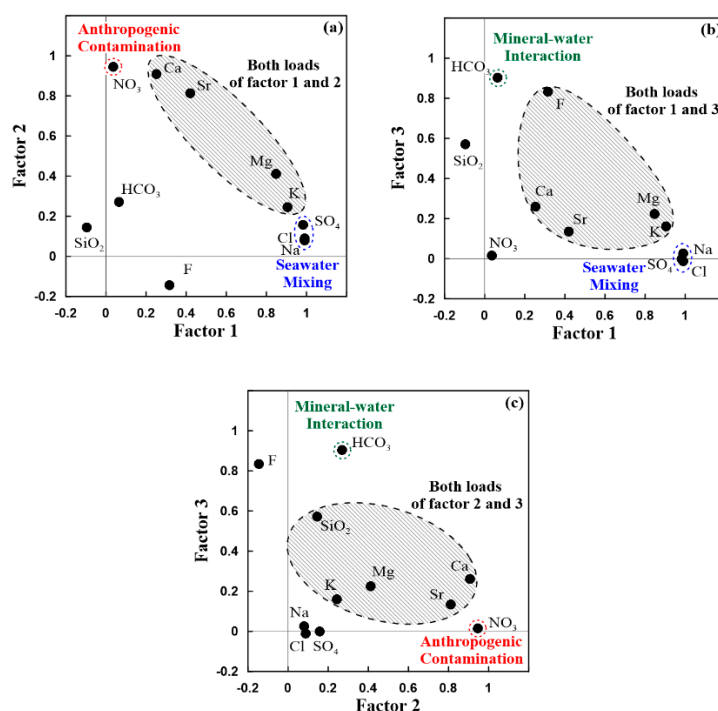
Figure 7. Distribution of variables among factors as produced by factor analysis. (**a**) Factor 1 vs Factor 2, (**b**) Factor 1 vs Factor 3, and (**c**) Factor 2 vs Factor 3.

Although Na, K and Mg are highly loaded at factor 1, of course, they can be partly derived from weathering process of feldspar ((Na, Ca, K) AlSi$_3$O$_8$), augite (CaMgSi$_2$O$_6$) and olivine ((Mg, Fe)$_2$SiO$_4$), which are major minerals of basaltic rocks. As SiO$_2$ has the highest load score (0.571) in factor 3, it also mainly originates from natural weathering process of above minerals.

It is not often that Ca and Sr highly loaded at factor 2 are originated from contamination sources. In case of high contaminated waters, however, they may be partly originated from pollution sources; e.g., a deicing material (Ca(Sr)Cl$_2$). As Sr shows very low concentration below 0.24 mg/L, it can occur as a minor substitute of Ca.

Fluorine can occur as a substitute of OH$^-$ in biotite rarely found in sedimentary rocks [39]. F of a low concentration below 0.45 mg/L has 0.315 load value in factor 1 and 0.833 load value in factor 3, respectively. This means that F also comes partly from sea water as well as mineral-water interaction as a major source.

4.3. Thermodynamic Equilibrium of Water-Mineral Interaction

The saturation index (SI) calculated by using the software program PHREEQC was used to better define the geochemical evolution reaction along a regional flow path of groundwater and spring water,

and to represent the thermodynamic equilibrium states between reactive minerals and groundwater and spring water in Jeju Island. SI values for certain minerals indicate the tendency for precipitation or the dissolution of these minerals: SI = 0 for thermodynamic equilibrium, SI > 0 for oversaturation (precipitation conditions), and SI < 0 for under-saturation (dissolution conditions). Here, the saturation index (SI) can be expressed in terms of ion activity product (IAP) and equilibrium constant (K) as follows: SI = IAP/K. Thermodynamic equilibrium can only indicate the potential for such mineral phase transfers. In reality, there are a number of kinetic reasons which may cause systems to behave differently than predicted [40,41]. Nevertheless, the saturation index can be useful for examining potential secondary phases and the dissolution of minerals of interest in aquifer system.

From the results of thermodynamic equilibrium calculation for given chemical data of groundwater and spring water samples, SI values were extracted for major minerals (feldspar, augite and olivine) of volcanic rocks in Jeju Island. For SI calculation, thermodynamic equilibrium constant data of albite, anorthite, tremolite, forsterite, diopside, and phlogopite, which are kinds of feldspar, augite, olivine and biotite groups as major minerals of basaltic and sedimentary rocks, were used from the values installed in the WATEQ4F data base.

The saturation indices between chemical data of all water samples and potential reactive minerals were statistically summarized according to the altitude of water samples (Table 5). The result indicates that most of waters were under-saturated with respect to major minerals except a few water samples of positive SI values with respect to tremolite. However, they were oversaturated with respect to illite, kaolinite and Ca-smectite as secondary minerals, which are randomly found at drilled cores and sedimentary rocks [42,43]. Except HCO_3 and F, which are indicative ions of factor 3, major ions such as Ca, Mg, Na, K, and SiO_2 have low load scores (0.025–0.570) at factor 3 indicating the main contribution by mineral-water interaction. These major ions are also to be main chemical composition of feldspar, augite, olivine and biotite in Jeju volcanic rocks. Then, thermodynamic under-saturation state in most of water samples with respect to above minerals correspond to low load scores of factor 3. Therefore, it is estimated that mineral-water interaction has a low contribution for the production of major ions such as Ca, Mg, Na, K, and SiO_2 in most of waters.

Table 5. Statistical saturation indices of chemical composition of groundwater (A) and spring water (B) with respect to major reactive minerals in Jeju Island.

Altitude (el. m)		Albite [1]	Anorthite [2]	Diopside [3]	Forsterite [4]	Phlogopite [5]	Tremolite [6]
(A)							
	Max.	−0.75	−3.89	−0.85	−6.50	−2.59	6.59
<100	Min	−20.4	−4.70	−7.53	−12.9	−12.4	−16.3
	Ave.	−2.79	−4.45	−5.15	−10.5	−8.47	−7.83
	Max.	−1.58	−4.34	−4.03	−9.42	−6.67	−3.84
100~400	Min	−3.73	−14.7	−10.5	−15.9	−17.8	−27.8
	Ave.	−2.07	−5.41	−6.37	−11.7	−10.4	−12.1
	Max.	−1.72	−4.52	−3.15	−8.61	−5.67	−0.99
400<	Min	−2.20	−4.91	−6.35	−11.7	−10.2	−12.0
	Ave.	−2.02	−4.77	−4.65	−10.0	−7.61	−6.00
(B)							
	Max.	−0.22	−3.56	−1.15	−6.57	−1.82	6.08
<100	Min	−2.22	−5.67	−8.96	−14.4	−14.5	−21.1
	Ave.	−1.39	−4.67	−6.41	−11.7	−10.1	−12.2
	Max.	−2.40	−4.72	−7.39	−12.6	−12.3	−15.9
100~400	Min	−2.63	−5.23	−8.05	−13.4	−13.1	−18.2
	Ave.	−2.52	−4.98	−7.72	−13.0	−12.7	−17.1
	Max.	−2.69	−5.35	−8.61	−14.1	−13.8	−20.2
400<	Min	−5.14	−8.53	−14.3	−19.6	−23.5	−40.5
	Ave.	−3.66	−6.45	−10.6	−15.9	−17.2	−27.3

[1]–[6] chemical formula: [1] $NaAlSi_3O_8$ [2] $CaAl_2Si_2O_8$; [3] $CaMgSi_2O_6$; [4] Mg_2SiO_4; [5] $KMg_3AlSi_3O_{10}(OH)_2$; [6] $Ca_2Mg_5Si_8O_{22}(OH)_2$.

Figure 8 shows the kriging contour map for SI values of all water samples with respect to major minerals using a semi-variogram method. The figure agrees with above explanation about an increasing trend of SI value from the central area including Mt. Halla to right and left coastal areas in Jeju Island. Whereas near-equilibrium state of some waters (maximum SI of −0.22) with respect to albite in a coastal area may results from high Na content due to sea water mixing, the waters are still under-saturated with respect to anorthite (Ca-plagioclase). The comparison of saturation indices indicates that groundwater and spring water for diopside and tremolite are evolved rather than those for forsterite and phlogopite. A few waters for diopside and tremolite are in near-equilibrium and oversaturated state. Considering the residence time (average 17 year) of groundwater in highly permeable aquifers of basaltic rocks [23], it is inferred that the reaction time is not enough to reach the equilibrium and oversaturation states through mineral-water interaction in a low temperature aquifer. The saturation indices have an increasing trend from higher altitude areas to lower altitude areas. Ignoring the effect of sea water mixing and anthropogenic input, this trend indicates that although groundwater and spring water dose not fully reach to thermodynamic equilibrium through mineral-water interaction, they have been hydrochemically evolved from higher mountain areas (recharge areas) to lower coastal areas (discharge areas) along regional flow paths.
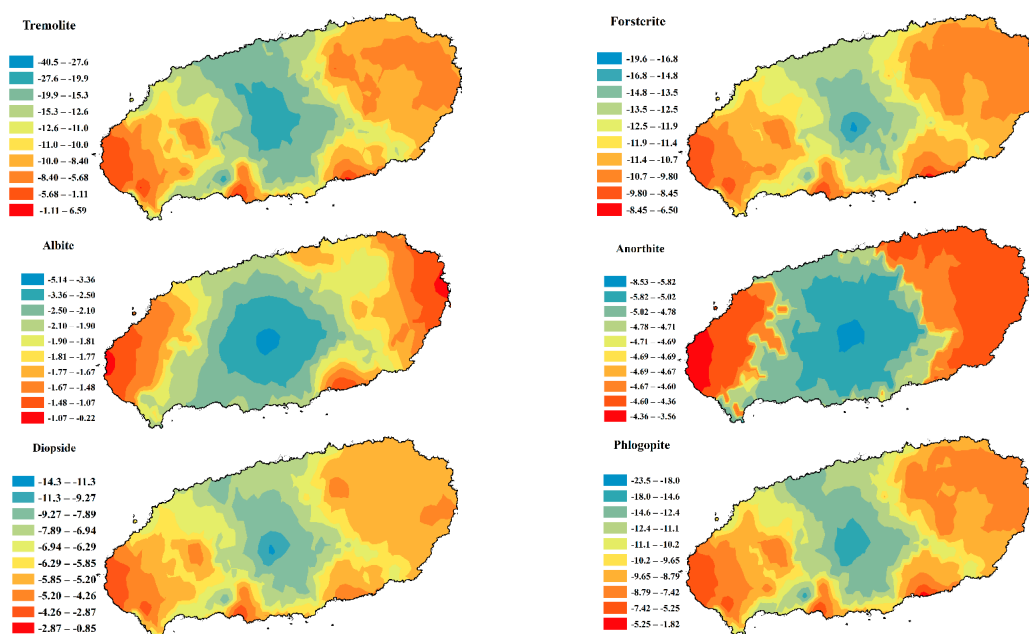

Figure 8. Kriging map of saturation indices between potential reactive minerals and chemical composition of groundwater and spring water samples in Jeju Island.

5. Conclusions

This study presented major contributions influencing the chemical composition of groundwater and spring water at Jeju Island. The main conclusions based on the results of this study are as follows:

(1) The pH and chemical composition of groundwater and spring water at Jeju Island show distinct differences according to their occurrence altitudes; higher saline and nitrate contents in lower areas. Box-Whisker and Piper diagrams indicate that the groundwater and spring water are divided as three chemical types through two different changing paths from an initial fresh water: 1) A fresh water type (Ca, Na-HCO$_3$), 2) a sea water mixing type (Na-Cl, SO$_4$), and 3) an anthropogenic contamination type (Ca-NO$_3$, Cl);

(2) By factor analysis, three main factors which can explain about 87 % of chemical variances of water samples were extracted. Na$^+$, Cl$^-$ and SO$_4^{2-}$ of factor 1, NO$_3^-$ of factor 2, and HCO$_3^-$ of factor 3, which have the highest load values are originally indicative ions of sea water mixing, contamination

and mineral-water interaction, respectively. Considering effective factor load values, other ions can be commonly derived by two or three original sources;

(3) Sea water intrusion in the eastern part of Jeju Island may be attributed to the distribution of Seogwipo Formation, which plays a role as an aquiclude preventing sea water intrusion in other coastal areas, under sea level. Nitrate contamination is closely related with agricultural activities, horse farms and municipal sewage, which are known as main pollution sources in coastal and mid-mountain areas at Jeju Island;

(4) The saturation indices from thermodynamic equilibrium calculation indicate that mineral-water interaction undergoes in aquifer except a few over-saturated waters with respect to major minerals of basaltic rocks. Thermodynamic under-saturation states in most of water samples with respect to feldspar, augite, olivine and biotite correspond to their load scores at factor 3. That is, mineral-water interaction has a relative low contribution for the origin of Ca, Mg, Na, K, and SiO_2 in most of waters. The non-equilibrium state in most of waters with respect to major minerals may be due to insufficient time for enough mineral–water interaction with a highly permeable aquifer.

References

1. Jeju Special Self-Governing Province Home Page. Available online: https://www.jeju.go.kr/open/stats/list/population.htm (accessed on 1 March 2020).

2. Ko, T.H.; Kang, J.M.; Lim, J.H. *Economic Effect Analysis of Tourism Industry in Jeju*, 1st ed.; Development Institute (JDI) Press: Jeju-si, Jeju-do, Korea, 2012; pp. 1–121. ISBN 978-89-6010-227-9 93320.

3. Lee, Y.D. Characteristics of groundwater quality by elevation in Cheju Island. *J. KoSES* **2001**, *5*, 65–75.

4. Koh, E.H.; Lee, S.H.; Kaown, D.; Moon, H.S.; Lee, E.; Lee, K.K.; Kang, B.R. Impacts of land use change and groundwater management on long-term nitrate-nitrogen and chloride trends in groundwater of Jeju Island, Korea. *Environ. Earth Sci.* **2017**, *20*, 76–176. [CrossRef]

5. Kim, G.B.; Kim, J.W.; Won, J.H.; Koh, G.W. Regional trend analysis for groundwater quality in Jeju Island—focusing on chloride and nitrate concentrations. *J. Korea Water Resour. Assoc.* **2007**, *40*, 469–483. [CrossRef]

6. IBM SPSS Statistic Version 25. 2017. Available online: https://www.ibm.com/kr-ko/products/spss-statistics/details (accessed on 22 October 2019).

7. PHREEQC. (Computer File) Water Chemistry, Computer Programs Geochemistry. Version 3.0; US Geological Survey (USGS): Denver, CO, USA, 1999. Available online: https://www.usgs.gov/software/phreeqc-version-3 (accessed on 22 October 2019).

8. Parkhurst, D.L. User's guide to PHREEQC–A computer program for speciation, reaction-path, advective-transport, and inverse geochemical calculations. *U.S. Geol. Surv.* **1995**, *8*, 1–143.

9. Lee, J.Y.; Lee, K.K. Use of hydrologic time series data for identification of recharge mechanism in a fractured bedrock aquifer system. *J. Hydrol.* **2000**, *229*, 190–201. [CrossRef]

10. Korea Institute of Geoscience and Mineral Resources (KIGAM). *Explanatory Note of the Jeju (Baekado, Jinnampo) Sheet (1:250,000)*; KIGAM Report; Geological and Mining Institute Korea: Seoul, Korea, 2000; pp. 1–59.

11. KIGAM. *Assessment of the Sustainable Yield on Groundwater in Jeju and Discovery of the Functional Groundwater*; KIGAM: Daejeon, Korea, 2011.

12. Korea Institute of Geoscience and Mineral Resources (KIGAM). *Geologic Report of the Jeju-Aewol Sheet (1:50,000)*; KIGAM Report; Geological and Mining Institute Korea: Seoul, Korea, 1998; pp. 1–290.

13. Korea Institute of Geoscience and Mineral Resources (KIGAM). *Geologic Report of the Moseulpo-Hanlim Sheet (1:50,000)*; KIGAM Report; Geological and Mining Institute Korea: Seoul, Korea, 2000; pp. 1–56.

14. Korea Institute of Geoscience and Mineral Resources (KIGAM). *Geologic Report of the Segwipo-Hahyori Sheet (1:50,000)*; KIGAM Report; Geological and Mining Institute Korea: Seoul, Korea, 2000; pp. 1–163.

15. Won, J.H.; Kim, J.W.; Koh, G.W.; Lee, J.Y. Evaluation of hydrogeological characteristics in Jeju Island, Korea. *Geosci. J.* **2005**, *9*, 33–46. [CrossRef]

16. Won, J.H.; Lee, J.Y.; Kim, J.W.; Koh, G.W. Groundwater occurrence on Jeju Island, Korea. *Hydrogeol. J.* **2006**, *14*, 532–547. [CrossRef]

17. Jeju Special Self-Governing Province. *Comprehensive Plans for Managing Water Resources in Jeju (2013–2022)*; Jeju Special Self-Governing Province: Jeju-do, Korea, 2018; pp. 1–366.

18. Koh, G.W. Characteristics of the Groundwater and Hydrogeologic Implication of the Seogwipo Formation in Cheju Island. Ph.D. Thesis, Busan National University, Busan, Korea, 20 July 1997.

19. Kim, B.S.; Hamm, S.Y.; Lee, C.M.; Ok, S.I.; Cha, E.J.; Ko, Y.S. Features of regional hydrogeology and groundwater distribution of volcanic rocks in Jeju Island. *J. Geol. Soc. Korea* **2011**, *47*, 263–273.

20. Hahn, J.S.; Hahn, K.S.; Kim, C.K.; Kim, N.J.; Hahn, C. Sustainable yield of groundwater resources of the Cheju Island. (In Korean with English abstract.). *J. Geol. Soc. Korea* **1994**, *1*, 33–50.

21. Choi, H.M.; Lee, J.Y.; Ha, K.; Kim, G.P. The study on time series analysis of groundwater data and groundwater recharge in Jeju Island. *J. Eng. Geol.* **2011**, *21*, 337–348, (In Korean with English abstract). [CrossRef]

22. Koh, D.C.; Cheon, S.H.; Park, K.H. Characterization of groundwater quality and recharge using periodic measurements of hydrogeochemical parameters and environmental tracers in basaltic aquifers of Jeju Island. *J. Soil Ground. Environ.* **2007**, *12*, 60–71.

23. Yoon, Y.Y.; Lee, K.Y.; Cho, S.Y.; Kim, Y.; Ko, K.S. The study of tritium analysis in Jeju Island groundwater. In Proceedings of the Korean Society of Analytical Sciences Conference, Seoul, Korea, 20–21 November 2008; p. 111.

24. Neal, C.; House, W.A.; Down, K. An assessment of excess carbon dioxide partial pressures in natural waters based on pH and alkalinity measurements. *Sci. Total Environ.* **1998**, *210–211*, 173–185. [CrossRef]

25. Neal, C.; House, W.A.; Jarvie, H.P.; Eatherall, A. The significance of dissolved carbon dioxide in major lowland rivers entering the North Sea. *Sci. Total Environ.* **1998**, *210–211*, 187–203. [CrossRef]

26. Appelo, C.A.J.; Postma, D. *Geochemistry, Groundwater and Pollution, A.A.*; Balkema Publishers: Rotterdam, The Nederland, 1996; ISBN 978-9054101062.

27. Nolan, B.T.; Stoner, J.D. Nutrients in groundwaters of the conterminous United States, 1992–1995. *Environ. Sci. Technol.* **2000**, *34*, 1156–1165. [CrossRef]

28. Stites, W.; Kraft, G.J. Nitrate and chloride loading to groundwater from an irrigated north–central U.S. sand–plain vegetable field. *J. Environ. Qual.* **2001**, *30*, 1176–1184. [CrossRef]

29. Chen, W.F.; Liu, T.K. Dissolved oxygen and nitrate of groundwater in Choshui Fan-Delta, western Taiwan. *Environ. Geol.* **2003**, *44*, 731–737. [CrossRef]

30. Babiker, I.S.; Mohamed, M.A.A.; Terao, H.; Kato, K.; Ohta, K. Assessment of groundwater contamination by nitrate leaching from intensive vegetable cultivation using geographical information system. *Environ. Int.* **2004**, *29*, 1009–1017. [CrossRef]

31. Erisman, J.W.; Sutton, M.A.; Galloway, J.; Kilmont, Z.; Winiwarter, W. How a century of ammonia synthesis changed the world. *Nat. Geosci.* **2008**, *1*, 636–639. [CrossRef]

32. Kurtzman, D.; Shapira, R.; Bar-Tal, A.; Fine, P.; Russo, D. Nitrate fluxes to groundwater under citrus orchards in Mediterranean climate: Observations, calibrated models, simulations and agro-hydrological conclusions. *J. Contam. Hydrol.* **2013**, *151*, 93–104. [CrossRef]

33. Usunoff, E.J.; Guzman-Guzman, A. Multivariate analysis in hydrochemistry: An example of the use factor and correspondence analyses. *Groundwater* **1989**, *27*, 27–34. [CrossRef]

34. Ritzi, R.W.; Wright, S.L.; Mann, B.; Chen, M. Analysis of temporal variability in hydrogeochemical data used for multivariate analyses. *Groundwater* **1993**, *31*, 221–229. [CrossRef]

35. Suk, H.; Lee, K. Characterization of a groundwater hydrochemical system through multivariate analysis: Clustering into groundwater zones. *Groundwater* **1999**, *37*, 358–366. [CrossRef]

36. Lee, J.Y.; Yang, J.S.; Han, M.; Choi, J.Y. Comparison of the microbiological and chemical characterization of harvested rainwater and reservoir water as alternative water resources. *Sci. Total Environ.* **2010**, *408*, 896–905. [CrossRef] [PubMed]

37. Cho, B.W.; Choo, C.O. Geochemical behavior of uranium and radon in groundwater of Jurassic granite area, Icheon, Middle Korea. *Water* **2019**, *11*, 1278. [CrossRef]

38. Johnson, R.A.; Wichern, D.W. *Applied Multivariate Statistical Analysis*, 3rd ed.; Prentice-Hall Inc.: Upper Saddle River, NJ, USA, 1992; ISBN 978-0130417732.

39. Apambire, W.B.; Boyle, D.R.; Michel, F.A. Geochemistry, genesis, and health implications of fluoriferous groundwaters in the upper regions of Ghana. *Environ. Geol.* **1997**, *33*, 13–24. [CrossRef]

40. Nordstrom, D.K.; Ball, J.W. Mineral saturation states in natural waters and their sensitivity to thermodynamic and analytical errors. *Sci. Geol. Bull.* **1989**, *42*, 269–280. [CrossRef]

41. Busby, J.E.; Plummer, N.; Lee, R.W.; Hanshaw, B.B. *Geochemical Evolution of Water in the Madison Aquifer in Parts of Montana, South Dakota, and Wyoming*; Professional Report Paper 1273-F; U.S. Geological Survey: Barton Rouge, MS, USA, 1991.

42. Hyun, W.H.; Hwang, J.Y.; Lee, J.Y.; Son, B.S.; Oh, J.H.; Yang, K.H.; Kim, K.H. Mineral composition of the Tamna Formation, Jeju Island, Korea. *Jour. Petrol. Soc. Korea.* **2016**, *25*, 335–348. [CrossRef]

43. Jeong, J.O.; Yoon, S.H.; Koh, G.W.; Joe, Y.J.; Hong, J.G.; Kim, J.J. Mineralogical and sedimentological characteristics of the U Formation underlying the volcanic strata in Jeju Island, Korea. *J. Geol. Soc. Korea.* **2016**, *52*, 389–403. [CrossRef]